Compressibility of Nuclear Matter from Shell Effects in Nuclei

M.M. Sharma
Physics Department, Kuwait University, Kuwait 13060

The compressibility of nuclear matter has received significant attention in the last decade and a variety of approaches have been employed to extract this fundamental property of matter. Recently, significant differences have emerged between the results of relativistic and non-relativistic calculations of breathing mode giant monopole resonance (GMR). This is due to a lack of understanding of the dynamics of GMR and of its exact relationship to the compression modulus of the infinite nuclear matter. Here, I present an alternative approach based upon nuclear shell effects. The shell effects are known to manifest experimentally in terms of particle-separation energies with an exceedingly high precision. Within the framework of the non-relativistic density-dependent Skyrme theory, it will be shown that the compressibility of nuclear matter has a significant influence on shell effects in nuclei. I will also show that 2-neutron separation energies and hence the empirical shell effects can be used to constrain the compressibility of nuclear matter.

Introduction

Shell effects manifest themselves in terms of the existence of magic numbers in nuclei. Inclusion of spin-orbit coupling in the shell model is known to account for the magic numbers[1)]. Shell effects are also found to appear more subtly e.g. as anomalous kink in the isotope shifts of Pb nuclei. It was shown that in the relativistic mean-field (RMF) theory, this kink appears naturally due to the inherent Dirac-Lorentz structure of nucleons[2)]. By including an appropriate isospin dependence of the spin-orbit potential in the density dependent Skyrme approach, the anomalous kink in the isotope shifts in Pb nuclei could be produced[3)].

The shell gaps at the magic numbers are known to produce important effects. Consequences due to the shell gaps are broadly termed as shell effects. The clearest manifestation of the shell effects can be seen in the pronounced dip in neutron and proton separation energies at the magic numbers in figures by Wapstra and Audi[4)] on the experimental separation energies all over the periodic table. Recently, shell effects have become focus of much attention[5,6)]. This is due to the reason that the shell effects in nuclei near the drip lines constitute an important ingredient to understand r-process abundances and heavy nucleosynthesis[7,8)].

In this talk, I focus upon 2-neutron separation energies to demonstrate that the shell efffects show a significant dependence upon the compressibility of nuclear matter. Using empirical data on the 2-neutron separation energies and thus implicitly the empirical shell effects, I will show that these data can be used to constrain the compressibility of nuclear matter. As the focus of this conference shows, the compression modulus K is an important fundamental property of the nuclear matter. It represents a cardinal point on the behaviour of equation of state (EOS) of the nuclear matter.

The compressibility of the nuclear matter has received a significant attention in the last decade and various approaches[9−11)] have been employed to extract the compression modulus. However, an unambiguous determination of the compression modulus of the nuclear matter has remained difficult due to a lesser sensitivity of the giant monopole resonance data to the compressibility[12,13)].

The Density-Dependent Skyrme Theory

Here I employ the density-dependent Skyrme theory[14)] to examine the shell effects. The Skyrme approach has generally been found to be very successful in providing ground-state properties of nuclei. The energy density functional used in the Skyrme approach is the standard one as given in Ref.[15)]. The corresponding energy per nucleon for the symmetric nuclear matter (with the Coulomb force switched off) is given by

$$(E/A)_\infty = k\rho^{2/3}(1+\beta\rho) + \frac{3}{8}t_0\rho + \frac{1}{16}t_3\rho^{1+\alpha} \qquad (1)$$

where $k = 75$ MeV.fm^2. The constant β is given in terms of the constants t_1 and t_2 and x_2 of the Skyrme force by

$$\beta = \frac{2m}{\hbar^2}\frac{1}{4}\Big[\frac{1}{4}(3t_1+5t_2) + t_2x_2\Big]. \qquad (2)$$

The constant β is also related to the effective mass m^* and the saturation density ρ_0 by

$$m/m^* = 1 + \beta\rho_0 \qquad (3)$$

The incompressibility (or the compression modulus) of the infinite nuclear matter is given as the curvature of the EOS curve and can be written as

$$K = 9\rho_0^2 \frac{d^2(E/A)(\rho)}{d\rho^2}\Big|_{\rho_0} \quad (4)$$
$$= -2k\rho_0^{2/3} + 10k\beta\rho_0^{5/3} + \frac{t_3}{16}\alpha(\alpha+1)\rho_0^{1+\alpha}$$

The parameters t_0, t_3 and α are usually obtained from the nuclear matter properties. The other parameters t_1, t_2 and various x parameters are obtained from fits to properties of finite nuclei. The strength W_0 responsible for the spin-orbit interaction is obtained by reproducing the spin-orbit splittings in nuclei such as ^{16}O and ^{40}Ca.

The Skyrme Forces

In order to show the effect of the incompressibility of nuclear matter on shell effects and consequently also on ground-state properties of nuclei, I have constructed a series of zero-range Skyrme forces. Experimental data on ground-state binding energies and charge radii of key nuclei such as ^{16}O, ^{40}Ca, ^{90}Zr, ^{116}Sn, ^{124}Sn and ^{208}Pb are taken into account in the least-square minimization. The ground-state properties in the Skyrme theory are calculated using the Hartree-Fock method.

With a view to vary K over a large range, the correlation between K and the saturation density is implicitly taken into account. This correlation has been summarized for Skyrme type of forces in Fig. 4 of Blaizot[9]. Accordingly, there exists an inverse correlation between the saturation density (Fermi momentum) and the compression modulus. Keeping this in mind, I have varied the saturation density ρ_0 over the range $0.140 - 170 fm^{-3}$ in steps of $.005 fm^{-3}$ as shown in Table 1.

The effective mass is fixed at 0.79. This value is required for being consistent with giant quadrupole resonance energies of heavy nuclei[15]. Eq. (3) then provides the value of β which can be used in eq. (2) to connect the coefficients t_1, t_2 and x_2. In order to do a systematic variation of the nuclear compressibility, I have kept the saturation binding energy fixed at a value of -16.0 MeV. This value is consistent with most nuclear mass models[16] and is close to physically acceptable values.

The coefficients α, t_0 and t_3 are determined by the eqs. (1), (4) and the saturation condition. However, we have allowed t_0 and t_3 to vary so that a fit to finite nuclei provides an incompressibility that is consistent with the inverse correlation. On the other hand, in an exhaustive computational exercise it is found that the violation of the above correlation results in bad fits for ground-state binding energies of key nuclei.

I have fixed x_1 and x_2 at zero for convenience. Given a value of β, the coeffients t_1 and t_2 in eq. (2) are obtained from the fits to the ground-state binding energies of finite nuclei. Thus, I have obtained various Skyrme parameter sets with incompressibility values K = 200, 220, 249, 270, 305, 327, 360 and 393 MeV, respectively. These forces encompass a broad range of physically plausible values of K. The nuclear matter properties of these forces are shown in Table 1. It can be seen that the force with K = 270 MeV was obtained for the sake of interpolation. Table 2 shows the total binding energies of some key nuclei obtained with the HF+BCS approach using the various Skyrme forces. It can be seen that all of these forces reproduce the total binding energies of the key nuclei from ^{16}O to ^{208}Pb very well.

Two-neutron Separation Energies and the Compressibility

I have selected the chain of Ni isotopes in order to probe the shell effects. As most Ni isotopes are known to be spherical and the experimental binding energies are known over a large range of Ni isotopes, the chain of Ni isotopes serves as an ideal test bench to probe the shell effects. Even-mass Ni isotopes from A=52 to A=70 are considered. This includes the neutron magic number N=28 (A=56) where we intend to investigate the shell effects due to the major shell closure.

With a view to obtain the ground-state properties of nuclei, we have performed spherical Skyrme Hartree-Fock calculations in coordinate space. Herein pairing is included using the BCS formalism with constant pairing gaps. Since nuclei under focus such as ^{56}Ni and ^{58}Ni are not far away from the stability line, the BCS scheme suffices to be a suitable mechanism for the pairing. Ground-state binding energies and *rms* charge and neutron radii for the Ni isotopes are calculated using the various Skyrme forces. The binding energies of nuclei are used to obtain the 2-neutron separation energies as

$$S_{2n}(Z,N) = B(Z,N) - B(Z,N-2), \quad (5)$$

where B represents the total binding energy of a nucleus.

As mentioned earlier, effects due to the shell gaps affect various nuclear properties besides the particle separation energies. First, the calculated charge radii of Ni isotopes are shown in Fig. 1. The charge radii show an increase with the incompressibility. Evidently, forces with the incompressibility about 200-250 MeV show a little dispersion in the values of the charge radii. However, above $K \sim 300$ MeV, there is a clear increase in the charge radii as a function of K and forces with a large incompressibility yield large values of charge radii for any given isotope. Inevitably, a large value of K hinders synthesis of nuclei with a radial extension which is diminuted

(compressed) contrary to that with a lower values of K. The empirical *rms* charge radii of ^{58}Ni, ^{60}Ni, ^{62}Ni and ^{64}Ni are taken from the compilation of Ref.[17] by solid circles. The values are 3.776, 3.815, 3.846 and 3.868 fm, respectively, obtained by folding the proton density distributions with the finite size 0.80 fm of protons. These results derive from experiments on muonic atoms. The *rms* charge radii deduced from the precision measurements in muonic atoms (taken from the recent compilation of Ref.[18] are 3.776, 3.813, 3.842 and 3.860 fm, respectively, which are almost identical to the previous compilation[17].

The empirical charge radii shown in Fig. 1 encompass the theoretical curves between K=270-327 MeV. Whereas the charge radius for ^{58}Ni points towards K=270 MeV, that for the heavier Ni isotopes is in the vicinity of K=327 MeV. Since the charge radii deduced from various methods have been obtained with a significant precision, these data could, in principle, be used to constrain the incompressibility. However, as there is still some model dependence in extraction of the charge radii, I would like to withhold any conclusions from this figure. On the other hand, the general trend of the experimental data points to a higher value of the compression modulus.

Figure 2 shows the corresponding *rms* neutron radii. The neutron radii show a monotonous increase with the mass number, with the exception of a slight kink at the magic number N=28. The change in the r_n values with K is similar to that for the charge radii, i.e. for lower values of K, there is a very little change in r_n with K. A significant change in the neutron radii, however, can be seen with large K values. The empirical *rms* neutron radii obtained from 800-MeV polarized-proton scattering experiment[17,19] for the isotopes ^{58}Ni and ^{64}Ni are shown in the figure by the solid points. The values lie between the curves for K=300 and K=327 MeV.

The 2-neutron separation energy S_{2n} for the Ni isotopes obtained with the various Skyrme forces are shown in Fig. 3. For the sake of clarity of the presentation, I have selected a set of the Skyrme forces in the figure. The dramatic fall in the S_{2n} curves is seen conspicuously for the nucleus just above the N=28 magic number. Such a kink in the S_{2n} values signifies the presence of the shell effects which arise from closure of a major shell. All the Skyrme forces produce such a kink in Fig. 3. However, the slope of the kink between A=56 (N=28) and A=58 (N=30) changes from one force to the other (as a function of the incompressibility K). The difference in the S_{2n} values of ^{56}Ni and ^{58}Ni can be taken as a measure of the shell effects. The force with the lowest incompressibility (K = 200 MeV) gives this difference as 6.59 MeV with a slope which is minimum amongst all the curves. This implies that the shell effects due to this force are the weakest one. As the K value increases, the corresponding difference shows a smooth increase and the ensuing steepness increases gradually. For the force with the highest incompressibility (K = 393 MeV), the difference amounts to 9.46 MeV. This difference is higher than the experimental difference[20] of 8.37 MeV. It implies that the shell effects show a strong dependence on the compression modulus K. Notwithstanding this correlation, the difference in the experimental values of S_{2n} can serve as a calibration for K. Consequently, the experimental difference and the slope is closest to the curve for K=270 MeV. Thus, on the basis of the empirical S_{2n} values, I infer that the incompressibility of nuclear matter lies in the neighbourhood of $K \sim 270$ MeV.

Shell Effects at the Neutron Drip-Line

Shell effects near the drip lines have been a matter of discussion of late[5,6]. It has been shown earlier that within the non-relativistic approaches of the Skyrme type, the shell effects near the drip lines and in particular near the neutron drip line are quenched[5]. This is contrary to that shown in the RMF theory by Sharma et al.[6], where the shell effects were observed to remain strong. Before such a debate is resolved, it is important to settle the issue of the shell effects near the stability line. Fig. 4 shows the 2-neutron separation energies for the Ni isotopes using the force SkP within the Hartree-Fock Bogolieubov approach[21]. The force SkP has been found to be successful in reproducing the ground-state properties of nuclei. The comparison of the SkP results with the experimental S_{2n} values shows that empirically there exist strong shell effects than predicted by the Skyrme force SkP. The compression modulus of the force SkP is about 200 MeV. Thus, the behaviour of the force SkP about the weak shell effects is consistent with the results from forces with low value of the incompressibility in Fig. 3. This suggests again that the shell effects in Ni are commensurate to a higher value of the compression modulus of the nuclear matter as inferred above.

How the shell effects behave along the neutron drip line as a function of the compression modulus can be visualized in Fig. 5. Here I have chosen the chain of Zr isotopes. This chain includes nuclei on both the sides of the magic number N=82 (A=122). The total binding energies obtained in the Hartree-Fock calculations with the various Skyrme forces are shown. For nuclei from A=116 (N=76) to A=122 (N=82), the total binding energy shows a steep increase in the value with all the forces. The forces with lower K show a stronger binding in general as compared to those with higher K, which is as expected. For nuclei above A=122, there is a striking difference in the way the binding energies progress with mass number. For the force with K = 200 MeV, the binding energy of nuclei heavier than ^{122}Zr shows an increase in the value with the mass number, implying that a further sequential addition of a pair of neutrons to the N=82 core does contribute to the binding energy. As the K value increases, the binding energy contribu-

tion from neutrons above N=82 starts diminishing. For K values 300 MeV and above, a stagnation is observed in the binding energies. Such a behaviour implies that the shell effects become stronger as the incompressibility increases. This is again an indication that the shell effects are strongly correlated to the incompressibility of the nuclear matter. Consequently, the incompressibility inferred from the ground-state data along the stability line suggests that the shell effects near the neutron drip line are strong. This is consistent with the strong shell effects about the neutron drip line as concluded in the RMF theory[6].

For nuclei near the drip lines, the HFB approach is considered to be more suitable than the HF+BCS one. However, the effects of the continuum are expected to be significant more for nuclei very near the drip line and in particular the observables which are most affected by coupling to the continuum are the *rms* radii. The total binding energies are known to show a little difference in the HF+BCS and HFB approaches. The main character of the shell effects is not altered by the inclusion of the continuum, as has been pointed out in Ref.[8] using the Skyrme force SIII. However, it will be interesting to see how a judicious choice of a force compatible with the experimental data as discussed above, will affect the r-process nucleosynthesis.

Summary and Conclusions

In the present work, I have shown that there exists a correlation between the shell effects and the compressibility of nuclear matter. The latter is shown to influence the shell effects significantly. Consequently, the 2-neutron separation energies show a strong dependence on the compression modulus. The ensuing correlation then provides a calibration for the compression modulus of nuclear matter. It is shown that using this correlation, the empirical data on the 2-neutron separation energies and thus implicitly the shell effects can be used to constrain the compressibility of nuclear matter. This procedure allows me to conclude that the incompressibility K should be within 270-300 MeV. This conclusion is also consistent with the experimental data on charge radii. A natural consequence of the present study is that the shell effects near the neutron drip line are predicted to be strong. This is in conformity with the strong shell effects observed at the neutron drip line in the RMF theory.

References

1) M.G. Mayer and J.H.D. Jensen, *Elementary Theory of Nuclear Shell Structure* (Wiley, New York, 1955).

2) M.M. Sharma, G.A. Lalazissis and P. Ring, Phys. Lett. **317**, 9 (1993).

3) M.M. Sharma, G.A. Lalazissis, J. König, and P. Ring, Phys. Rev. Lett. **74** 3744 (1994).

4) C. Borcea, G. Audi, A.H. Wapstra and P. Favaron, Nucl. Phys. **A565** 158 (1993).

5) J. Dobaczewski et al., Phys. Rev. Lett. **72** 981 (1994); ibid **73** 1869 (1994).

6) M.M. Sharma, G.A. Lalazissis, W. Hillebrandt and P. Ring, Phys. Rev. Lett. **72** 1431 (1994); ibid **73** 1870 (1994).

7) K.-L. Kratz et al., Astrophys. J. **403** 216 (1993).

8) B. Chen et al., Phys. Lett. **B355** 37 (1995).

9) J.P. Blaizot, Phys. Rep. **64** 171 (1980).

10) M.M. Sharma et al., Phys. Rev. **C38** 2562 (1988).

11) M.V. Stoitsov, P. Ring and M.M. Sharma, Phys. Rev. **C50** 1445 (1994).

12) J.M. Pearson, Phys. Lett. **B271** 12 (1991).

13) S. Shlomo and D.H. Youngblood, Phys. Rev. **C47** 529 (1993).

14) D. Vautherin and D.M. Brink, Phys. Rev. **C7** 296 (1973).

15) M. Brack, C. Guet and H.B. Hakansson, Phys. Rep. **123** 275 (1985).

16) P. Möller, J.R. Nix, W.D. Myers and W.J. Swiatecki, At. Data Nucl. Data Tables **59** 185 (1995).

17) C.J. Batty, E. Friedmann, H.J. Gils and H. Rebel, Adv. Nucl. Phys. **19** 1 (1989).

18) G. Fricke et al., Atomic Data and Nuclear Data Tables **60** 178 (1995).

19) L. Ray, Phys. Rev. **C19** 1855 (1979).

20) A.H. Wapstra and G. Audi, Nucl. Phys. **A565** 1 (1993).

21) J. Dobaczewski et al., Nucl. Phys. **A422** 103 (1984) and private communication (1994).

Table 1. The nuclear matter properties of the various Skyrme interactions. The saturation energy E/A has been fixed at -16.0 MeV and the effective mass m* has been kept at 0.79.

Force	ρ_0 (fm^{-3})	K (MeV)	a_{sym} (MeV)
I	0.140	393	38.0
II	0.145	360	32.4
III	0.150	327	32.5
IV	0.155	305	32.3
V	0.160	249	32.5
VI	0.165	220	32.0
VII	0.170	200	31.8

Table 2. The total binding energy (MeV) of nuclei obtained from the HF+BCS calculations with the Skyrme interactions. The empirical values (exp.) are shown for comparison.

		K (MeV)						
Nucleus	exp.	393	360	327	305	249	220	200
^{16}O	-127.6	-127.5	-127.5	-125.5	-127.5	-127.5	-127.6	-127.7
^{40}Ca	-342.0	-342.5	-342.4	-342.2	-342.0	-342.4	-342.5	-342.4
^{90}Zr	-783.9	-786.6	-786.0	-785.6	-785.2	-785.3	-784.6	-784.3
^{116}Sn	-988.7	-989.2	-988.1	-987.0	-986.1	-986.1	-985.5	-985.4
^{120}Sn	-1020.5	-1021.3	-1020.1	-1019.6	-1019.3	-1019.1	-1018.9	-1018.9
^{124}Sn	-1050.0	-1051.0	-1049.7	-1050.0	-1050.5	-1049.9	-1050.1	-1050.3
^{208}Pb	-1636.5	-1636.5	-1635.7	-1636.0	-1636.5	-1636.2	-1637.2	-1637.0

Figure Captions

Fig. 1. Charge radii for Ni isotopes with various Skyrme forces. The experimental values for a few nuclei from Refs.[17,18] are shown by solid dots.

Fig. 2. Neutron radii for Ni isotopes with various Skyrme forces. The experimental values for ^{58}Ni and ^{64}Ni from Refs.[19] are shown by solid dots.

Fig. 3. Two-neutron separation energy S_{2n} for Ni isotopes obtained with various Skyrme forces. Comparison with the experimental data from Ref.[20] is also made.

Fig. 4. Total binding energy of Zr isotopes near the neutron drip line calculated with the Skyrme forces.

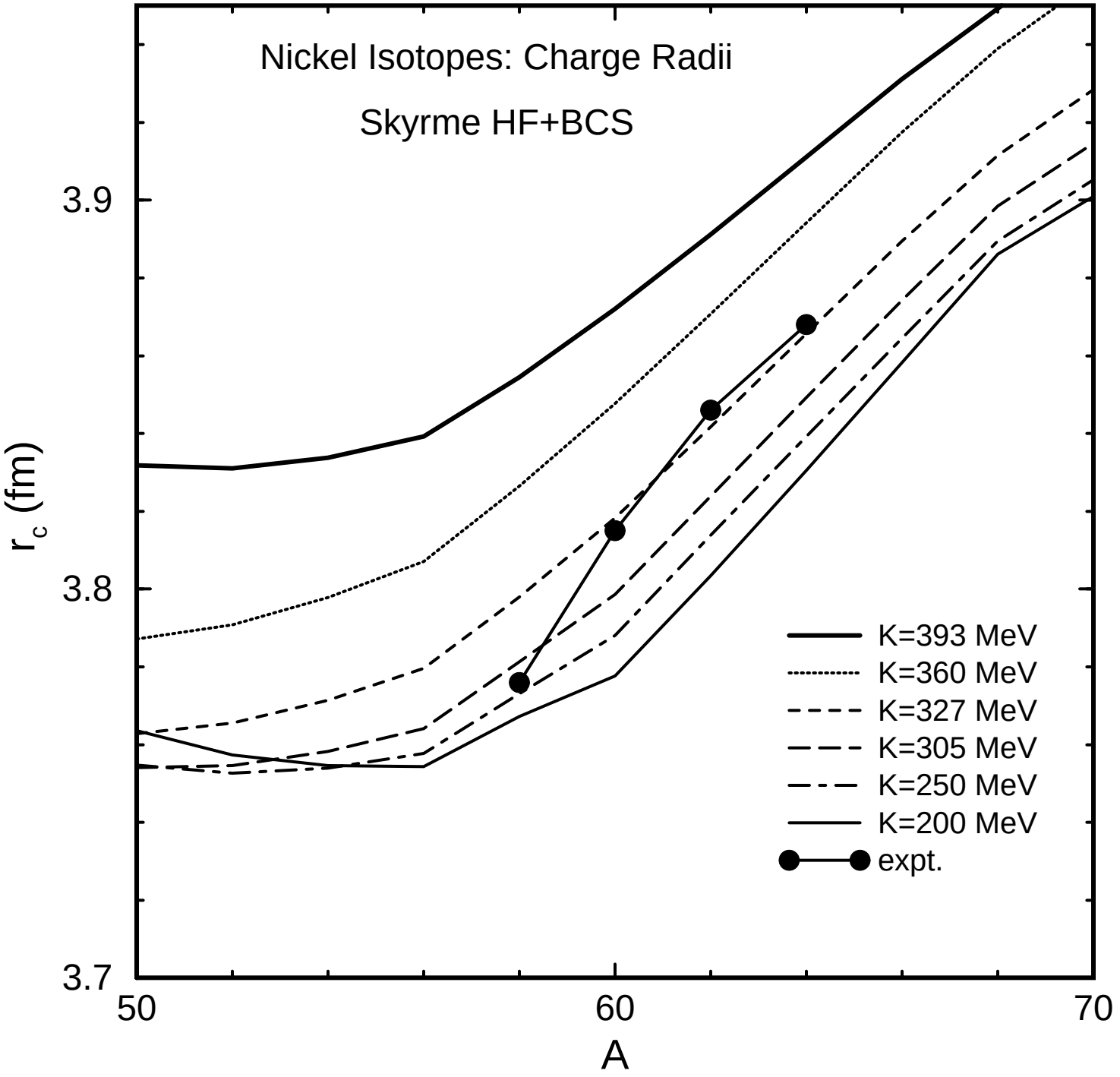
Nickel Isotopes: Charge Radii
Skyrme HF+BCS
3.9
3.8
3.7
r_c (fm)
50
60
70
A
K=393 MeV
K=360 MeV
K=327 MeV
K=305 MeV
K=250 MeV
K=200 MeV
expt.

Fig.1.

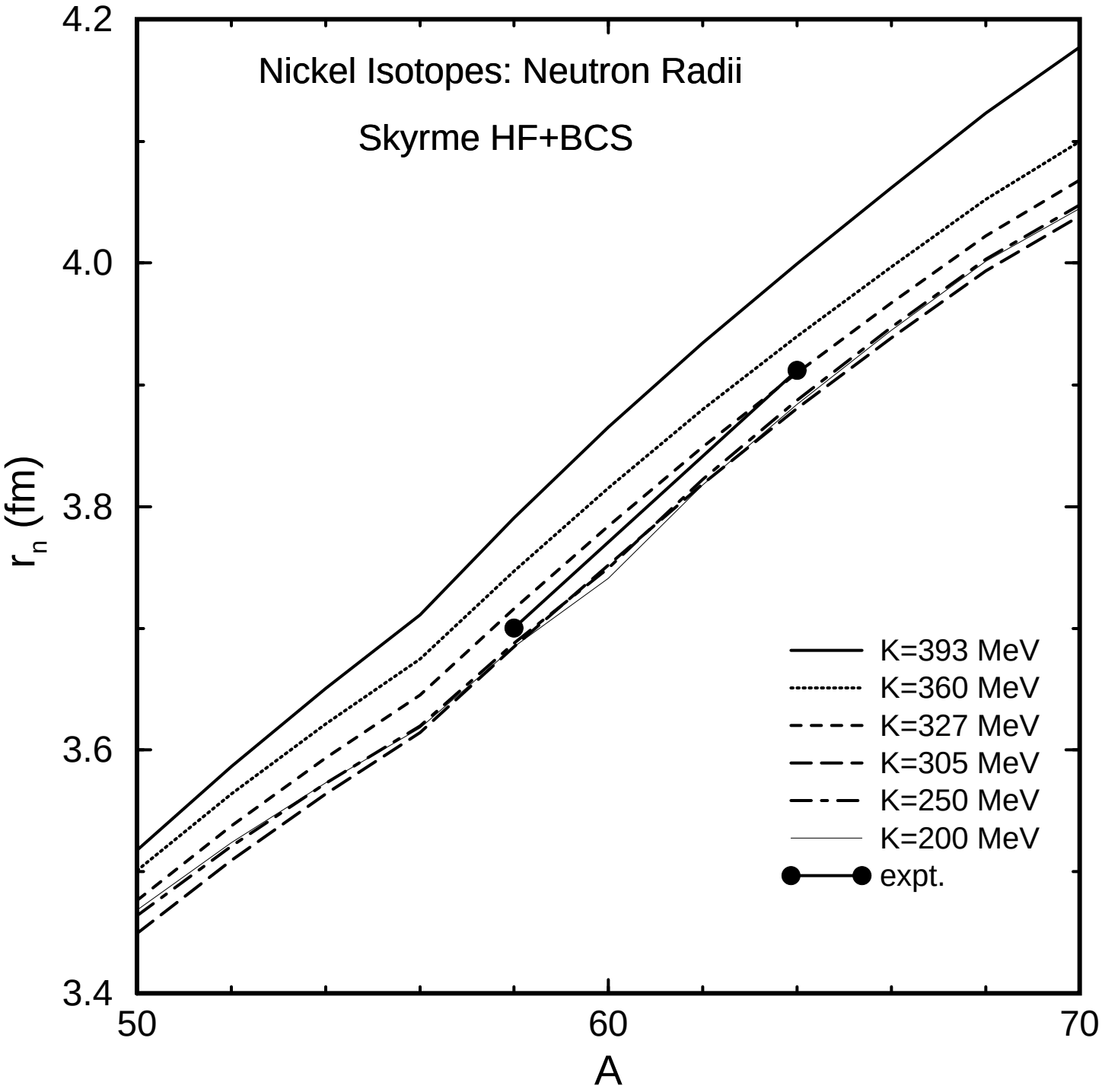
Nickel Isotopes: Neutron Radii
Skyrme HF+BCS
4.2
4.0
3.8
3.6
3.4
r_n (fm)
50
60
70
A
K=393 MeV
K=360 MeV
K=327 MeV
K=305 MeV
K=250 MeV
K=200 MeV
expt.

Fig. 2.

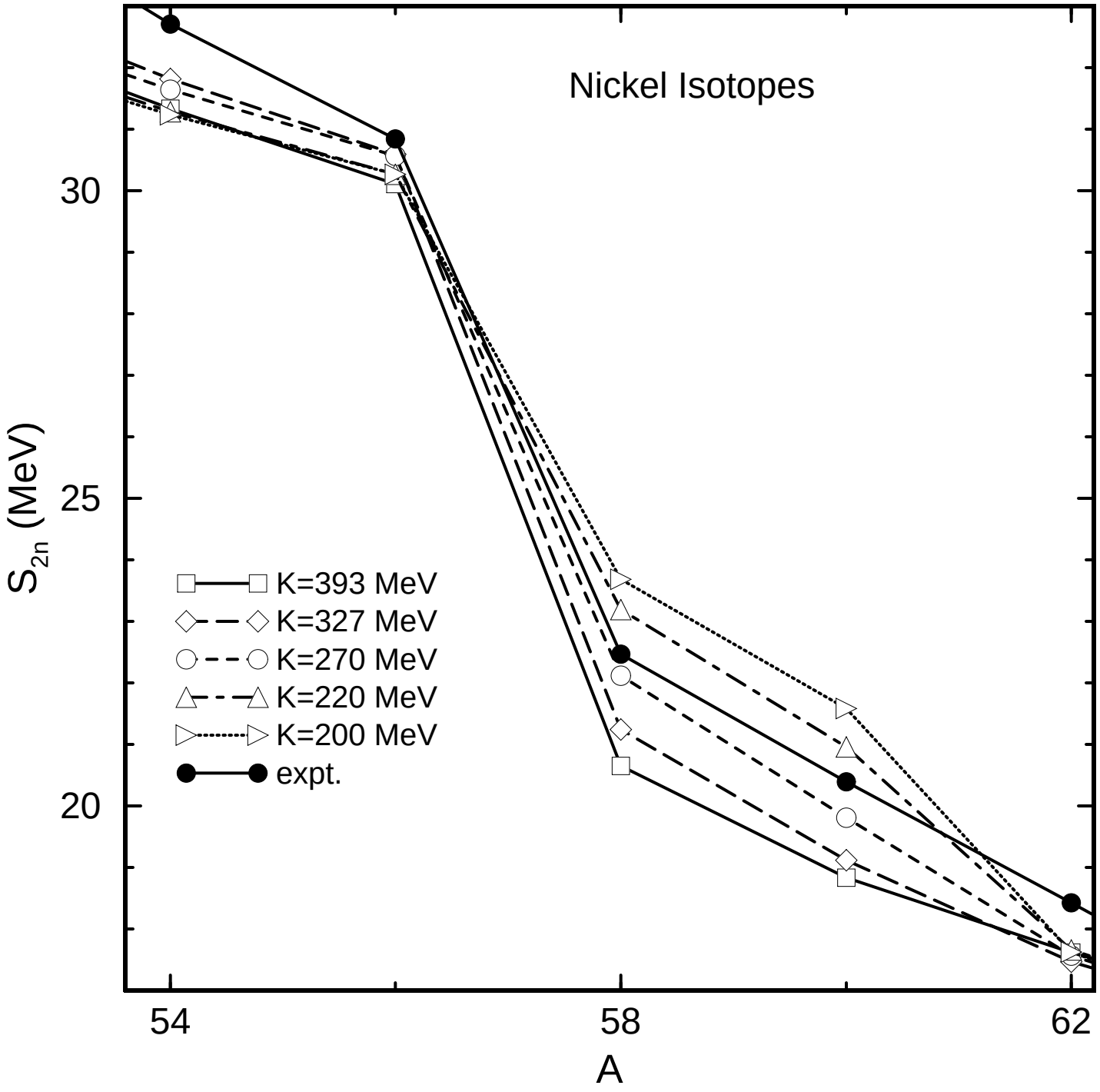
Nickel Isotopes
30
25
20
S_{2n} (MeV)
54
58
62
A
K=393 MeV
K=327 MeV
K=270 MeV
K=220 MeV
K=200 MeV
expt.

Fig. 3.

Fig. 4.

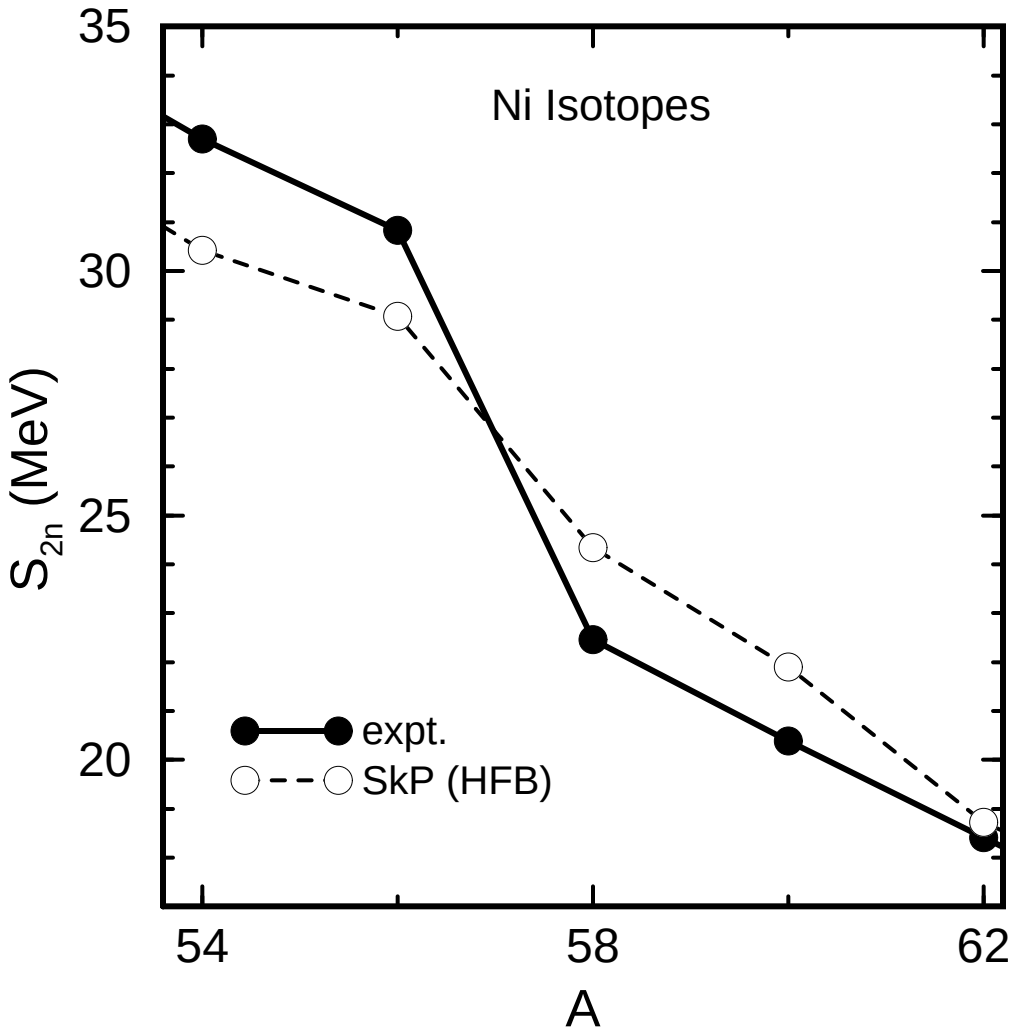

Fig. 5.

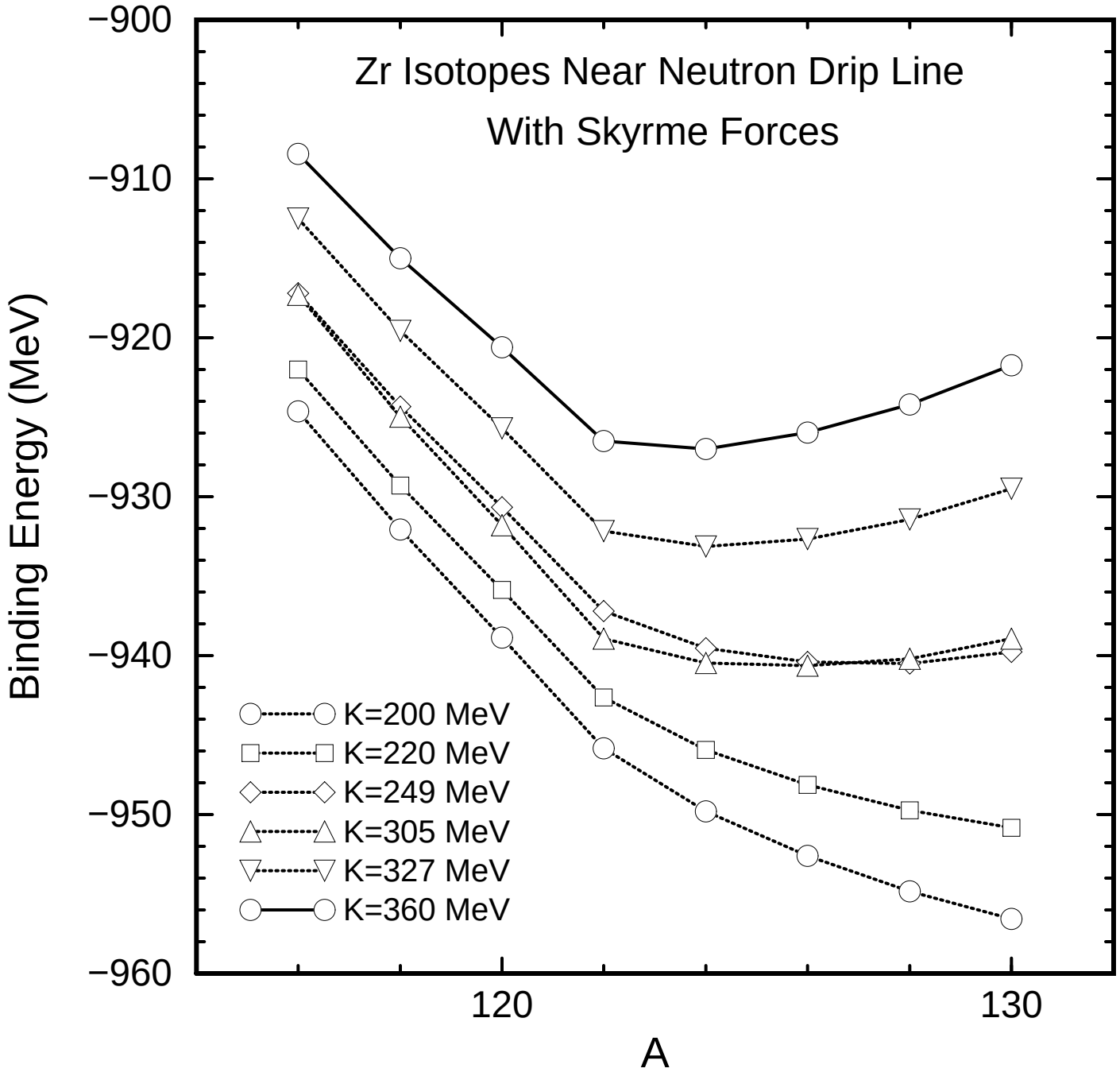
Zr Isotopes Near Neutron Drip Line
With Skyrme Forces
Binding Energy (MeV)
−900
−910
−920
−930
−940
−950
−960
120
130
A
K=200 MeV
K=220 MeV
K=249 MeV
K=305 MeV
K=327 MeV
K=360 MeV